

Timothy Michael Gallagher

A new paleothermometer for forest paleosols and its implications for Cenozoic climate

Submitted for Publication in:

Geology

in lieu of thesis in partial fulfillment of the requirements for the degree of

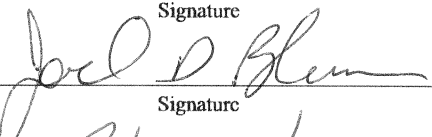
Master of Science in Geology

Department of Earth and Environmental Sciences

The University of Michigan



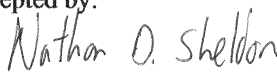
Signature



Signature



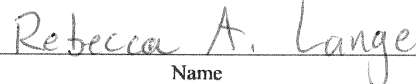
Department Chair Signature

Accepted by:


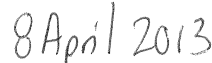
Name



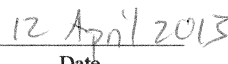
Name



Name



Date



Date

I hereby grant the University of Michigan, its heirs and assigns, the non-exclusive right to reproduce and distribute single copies of my thesis, in whole or in part, in any format. I represent and warrant to the University of Michigan that the thesis is an original work, does not infringe or violate any rights of others, and that I make these grants as the sole owner of the rights to my thesis. I understand that I will not receive royalties for any reproduction of this thesis.

Permission granted.

Permission granted to copy after: _____

Permission declined.



Author Signature

A new paleothermometer for forest paleosols and its implications for Cenozoic climate

Timothy M. Gallagher and Nathan D. Sheldon

Department of Earth and Environmental Sciences, University of Michigan, 2534 CC Little, 1100 N. University Ave, Ann Arbor, Michigan 48109, USA

ABSTRACT

Climate is a primary control on the chemical composition of paleosols, making them a potentially extensive archive applicable to problems ranging from paleoclimate reconstruction to paleoaltimetry. However, the development of an effective, widely-applicable paleosol temperature proxy has remained elusive. This is attributable to the fact that various soil orders behave differently due to their respective physical and chemical properties. Therefore, by focusing on an individual order or a subset of the twelve soil orders whose members exhibit similar process behavior, a better constrained paleothermometer can be constructed. Soil chemistry data were compiled for 158 modern soils in order to derive a new paleosol paleothermometry relationship between mean annual temperature and a paleosol weathering index (PWI) that is based on the relative loss of major cations (Na, Mg, K, Ca) from soil B horizons. The new paleothermometer can be applied to clay-rich paleosols that originally formed under forest vegetation, including Inceptisols, Alfisols, and Ultisols, and halves the uncertainty relative to previous approaches. A case study using Cenozoic paleosols from Oregon shows that paleotemperatures produced with this new proxy compare favorably with paleobotanical temperature estimates. Global climatic events are also evident in the Oregon paleosol record,

including a 2.8 °C drop across the Eocene-Oligocene transition comparable to marine records, and a Neogene peak temperature during the Mid-Miocene Climatic Optimum.

INTRODUCTION

The structure and chemical composition of paleosols provide a valuable continental paleoclimate archive, because climate is one of the primary factors controlling soil formation (e.g., Jenny, 1941). Paleosols are found throughout the geologic record, reaching further back in time than other paleoclimate archives such as ice cores, and are preserved more commonly than paleobotanical assemblages. Attempts at quantifying distinct climate processes using paleosols have been met with varying degrees of success. While a number of proxies have been developed that effectively estimate paleo-rainfall for most paleosols (Sheldon et al., 2002; Retallack, 2005; Nordt and Driese, 2010a), the development of a quantitative temperature proxy for paleosols applicable to more than single soil orders (e.g., Sheldon, 2006) has proven more difficult. At the same time, paleosol-derived paleotemperature estimates have been used for a number of applications ranging from paleoclimate(e.g, Retallack, 2007) to paleoelevation (e.g., Takeuchi et al., 2007) studies, making any substantial paleothermometry improvement applicable to a variety of fields.

Sheldon et al. (2002) identified a modest relationship in modern soils between temperature and the molar ratio of Na and K to Al. While significant, the resultant climofunction has an error of ± 4.4 °C and effective range of 8–22 °C, which limits the utility of this proxy in that it is only applicable for a relatively narrow window of climatic conditions and cannot distinguish small climatic shifts. The $\delta^{18}\text{O}$ of pedogenic carbonate in paleosols has also been proposed as a temperature proxy (Dworkin et al., 2005). However, many paleosols lack pedogenic carbonate, and this proxy is complicated by both the variability of meteoric $\delta^{18}\text{O}$

across isotherms and the potential for evaporation changing the $\delta^{18}\text{O}$ of soil water in carbonate producing soils (Sheldon and Tabor, 2009). Another paleosol temperature reconstruction method uses paired measurements of $\delta^{18}\text{O}$ and δD from a single mineral, such as goethite, smectite, or kaolinite, yet these estimates rely on the assumption that the meteoric water line has not changed over geologic time (Delgado and Reyes, 1996; Yapp, 2000; Sheldon and Tabor, 2009).

Measuring $\delta^{18}\text{O}$ on mineral pairs, such as hematite and phyllosilicates, shows promise for reconstructing past temperatures, but to date there are few studies employing this method (Tabor, 2007).

All of the studies mentioned above strove for a paleothermometer that can be used on all paleosols, yet different soil orders and vegetation types behave differently due to their unique physical and chemical properties (e.g., clay content), making soil order specific proxies (Sheldon, 2006; Nordt and Driese, 2010a) or plant-functional group specific proxies more effective. This study proposes a paleothermometer for three soil orders found in forest ecosystems: Alfisols, Ultisols, and Inceptisols. Alfisols and Ultisols are well-developed soils that typically form under forest vegetation and are characterized by clay-rich argillic (Bt) horizons that are base-rich and base-poor, respectively. Inceptisols are moderately developed soils that have developed cambic (Bw) horizons, but not argillic horizons. While Inceptisols are not formed exclusively under forest vegetation, their inclusion in this study enables the application of this proxy to both moderately and well-developed paleosols. Soils from these three orders are widely distributed today and account for approximately one-third of non-ice-covered land on the planet (Buol et al., 2011). They are ubiquitous in the geologic record as well, with all three orders present since the Carboniferous and easily identifiable based upon readily preserved features (e.g., horizonation; Retallack, 2001).

MATERIALS AND METHODS

Soil chemistry data were compiled from three different studies of modern soils. Marbut (1935) includes whole-soil elemental data from 94 forest soils that are widely dispersed across the United States. The second source, Rasmussen and Tabor (2007), includes chemical data for 10 forest soils in California and Baja California. The final source, Nordt and Driese (2010b), contains soil chemistry data for 14 Vertisols in Texas, Alabama, and New Mexico. By convention, the chemical data from these three studies were converted from weight-percentages of oxides to a molar ratio. Means of B-horizon data were used because the long formation time necessary for horizon development allows equilibrium processes to predominate and precludes overprinting by short-lived climatic events such as ENSO (Sheldon and Tabor, 2009). Both Rasmussen and Tabor (2007) and Nordt and Driese (2010b) published climatic data associated with each soil sample; however, no climatic data was included in Marbut (1935). Thus, the Marbut soil chemical data were paired with mean annual temperature (MAT) normals from the closest NOAA weather station (National Climatic Data Center, 2002).

WEATHERING INDEX

The paleosol weathering index (PWI) used here is a modified version of the index of weathering originally published by Parker (1970). The PWI is based on the fact that certain major elements (Na, K) are more susceptible to chemical weathering and subsequent leaching in a soil than others (Mg, Ca) at a molecular level. It approximates this susceptibility to weathering by assuming that a completely ionic bond exists between the cations and O²⁻, allowing for the calculation of their relative bond strengths. The relative molar abundances of these cations in a sample are then divided by their respective relative bond strengths and percent ionic character and summed to give the following expression:

$$PWI = 100 * (4.20 * Na + 1.66 * Mg + 5.54 * K + 2.05 * Ca). \quad (1)$$

The relative bond strengths were calculated using an effective ionic radius of 1.26 Å for O²⁻. A term for the percent ionic character of each cation was also included to account for their varying degrees of covalency. For example, Na has a calculated relative bond strength of 1.32 and a percent ionic character of 0.79. The inverse of the product of these two values gives a coefficient for Na of 4.20 (see Table DR1 in the GSA Data Repository¹ for the exact values used to derive the coefficients). In this index, an element with a higher coefficient is considered easier to leach from a soil. While Na and K are found in minerals generally considered relatively resistant to weathering, such as alkali-feldspars, it has been shown that these weakly bonded cations can be preferentially leached from a feldspar while the aluminum-silica framework remains intact (Chou and Wollast, 1984).

The PWI effectively captures the development of a soil's chemical composition away from that of its parent material (Fig. 1). A high PWI value indicates a less-developed soil whose chemical composition is similar to that of its parent material. Conversely, a low PWI value is indicative of a well-developed soil that is depleted of alkali and alkaline-earth elements. This index reflects the fact that of these three soil orders, Ultisols tend to be the most leached of major base cations and Inceptisols the least (Fig. 1). With the exception of the least developed Inceptisols, all of the soils in this data set have a PWI value that is distinct from parent rock material.

PWI PALEOTHERMOMETER

The relationship between the PWI and MAT values for each of the soils is used to derive a new paleothermometer. The modern soil PWI values are plotted against their respective MAT values in Figure 2. Soils formed in areas with a MAT under 6 °C were not included in the

regression (Fig. 2) because weathering indices tend to behave at a much slower rate below this threshold (Óskarsson et al., 2012). A regression through this data set produces the following paleothermometry relationship, which has a standard error of ± 2.1 °C:

$$T(\text{°C}) = -2.74 * \ln(\text{PWI}) + 21.39. \quad (2)$$

A logarithmic regression ($r^2 = 0.57$, standard error [S.E.] = ± 2.1 °C) through the data set produced a better fit than a linear regression ($r^2 = 0.50$, S.E. = ± 2.3 °C), and is a more logical choice because chemical reaction rates in soils behave nonlinearly with respect to temperature (Turk et al., 2012). Furthermore, it is also logical for the fit to reach an asymptote near zero because it is impossible to have a negative PWI value. This proxy has an arithmetic range of 8–36 °C, including error and using PWI values of 0.01 and 60. The fit is not improved by considering PWI depth-profile relationships or by a simple B-horizon minus parent material index. The relationship between the PWI and mean annual precipitation was also evaluated, but only a weak correlation exists ($r^2 = 0.20$; Figure DR1).

This paleothermometer should not be used on paleosols with a PWI over 60, because such paleosols are essentially indistinguishable from unweathered parent materials (Fig. 1). The PWI value of the paleosol B-horizon should also be lower than the PWI value of the parent material. It is also essential to remove any carbonate from samples before analysis, because the presence of soil carbonates will result in an artificially high PWI value that is not reflective of the MAT. However, any acid treatment of samples may potentially leach cations loosely bound to phyllosilicate minerals, effectively producing a maximum MAT estimate.

The PWI-paleothermometer is specifically designed for clay-rich forest paleosols, which correspond to Argillisols and some Protosols (e.g., argillic Protosols) in the Mack et al. (1993) paleosol classification scheme. It does not apply to other soil orders, which have distinct

properties resulting in different rates of cation leaching. For example, no significant relationship exists between PWI and MAT in Vertisols (Figure DR2), which are comparably clay-rich (dominated by shrink-swell clays) to forest soil orders, but which form under strongly seasonal climates and under grassland and forb vegetation. The lack of a relationship can be attributed to the fact that cation leaching tends to be more inhibited in Vertisols than in forest soils, allowing for smectite to remain stable (Buol et al., 2011). Icelandic Andisols also exhibit a distinct cation leaching behavior in which Na^+ and K^+ are more easily retained than Ca^{2+} and Mg^{2+} , which can be attributed to the poorly crystalline nature of the dominant clay minerals in the soils, allophane, ferrihydrite, and imogolite (Óskarsson et al., 2012). Before applying the PWI-paleothermometer, it is critical to identify specific soil features indicative of a forest paleosol, such as a Bw or Bt horizon and clay coatings on peds or detrital grains, rather than relying solely on clay content. Because the calibration of this proxy also excludes soils with a MAT below 6°C, any evidence of frost-wedging (i.e., Gelisol-like paleosols) precludes the use of this paleothermometer.

Although the PWI-paleothermometer is calibrated using mid-latitude modern forest soils with MATs ranging between 6 and 23°C, it is also applicable to paleosols formed under greenhouse conditions. Warmer worlds are characterized by increased equability and modified latitudinal distribution of environments rather than simply having uniformly higher temperatures. For example, using a coupled ocean-atmosphere general circulation model with a dynamic vegetation component to evaluate Late-Cretaceous greenhouse climate, Zhou et al. (2012) found in high- CO_2 experiments (10x to 16x pre-industrial levels) that forest vegetation expanded poleward and that continental surface MAT ranged from 6–24°C at latitudes above 30°. This temperature range is consistent with the calibration dataset, suggesting that the PWI-paleothermometer can be applied to paleosols formed at mid to high-latitudes in a greenhouse

world as well as to icehouse world conditions with environmental distributions similar to the modern calibration data.

OREGON CASE STUDY

To evaluate this new temperature proxy, MAT estimates were recalculated for the Retallack (2007) Oregon paleosol data set (Fig. 3). This data set consists of B horizon major-element data from 161 paleosols formed on volcanic and volcaniclastic parent materials in western Oregon and southeastern Washington, and which range in age from the mid-Eocene (45 Ma) through the Quaternary. The ages of these paleosols are very well constrained due to three types of age control: direct dating of ash beds, biostratigraphy, and magnetostratigraphy.

The record was compared with reconstructed temperatures from paleobotanical studies in order to evaluate if these new MAT values are in agreement with other proxies. Most of the published temperature estimates based on Cenozoic paleofloras from Oregon have used the CLAMP method. While CLAMP has flaws and tends to underestimate paleotemperature (Peppe et al., 2011), these estimates do offer a relative benchmark for comparison. Paleobotanical temperature estimates from Eastern Oregon suggest a temperature drop of ~3 °C between 34.4 and 30.6 Ma (Meyers, 2003). This compares favorably with the PWI-calculated paleosol temperature drop of 3.5 °C during the same time period (Fig. 3).

One of the main problems with the original MAT estimates from the Oregon paleosol data set (Retallack, 2007) is that reconstructed temperatures fall to as low as 6.2 °C in the Late Oligocene and 4.7 °C in the Early Miocene when using the salinization paleothermometer of Sheldon et al. (2002). These temperatures are significantly colder than regional paleobotanical estimates, with an estimate of 15.5 °C coming from the Late Oligocene (~24–27 Ma) Yaquina flora of coastal Oregon, and an estimate of 12 °C from the Early Miocene (~18–22 Ma) Eagle

Creek flora of northwest Oregon (Wolfe, 1994). The PWI-paleothermometer better resolves this discrepancy, with calculated temperatures falling only to 10.5 ± 2.1 °C during this period (Fig. 3). The regional paleobotanical and PWI temperature records continue to parallel each other throughout the Miocene, peaking during the Middle Miocene before a general decline (Wolfe, 1994).

Another point available for comparison is the modern soil in the Oregon paleosol data set located near Helix, OR. Averaging data from the two closest (~20 km) NOAA weather stations in Milton-Freewater, OR and Pendleton, OR yields a modern MAT of 11.2 °C (National Climatic Data Center, 2002). The PWI-paleothermometer produces a calculated MAT of 11.0 °C, which is indistinguishable given the measurement error in both types of data.

The stacked deep-marine oxygen isotope curve provides a record of global climate trends to compare with the regional continental temperature record from Eastern Oregon (Fig. 3). Although it is difficult to compare the exact magnitude of temperature changes from the isotope curve due to changes in ice-volume, the timing of the trends are remarkably similar. The continental paleotemperature record captures trends such as cooling across the Eocene-Oligocene (E-O) boundary. Between 34.3 and 33.3 Ma, the Oregon paleosols record a temperature drop of 2.8 °C, while the deep marine $\delta^{18}\text{O}$ record increases by 0.8‰ (Fig. 3). Recent combined model-data results predict a benthic oceanic cooling of 3–5 °C during the same time period (Liu et al., 2009), comparable to the paleosol-derived record. This cooling is followed by Late Oligocene warming that peaks at 24.5 Ma according to the marine record, which is synchronous with the maximum continental Late Oligocene MAT of 11.4 °C. After this event, the Oregon paleosol record reaches its Neogene maximum of 12.7 °C at 15.7 Ma, which is contemporaneous with the Mid-Miocene Climatic Optimum (Fig. 3). Both records are then characterized by general cooling

through the Pliocene and Quaternary. The one apparent difference between the two records is that while the marine isotope record documents a gradual cooling of deep marine water throughout the Middle to Late Eocene, terrestrial temperatures in Oregon appear to have risen. However, the Oregon record in the Eocene is very low resolution making it difficult to assess the nature of this contrast.

CONCLUSIONS

As parent material chemically weathers during soil development, major cations are released and eventually leached from the soil. Na^+ and K^+ tend to be more easily leached than Ca^{2+} and Mg^{2+} , and this can be quantified using the PWI. In clay-dominated forest soils, there is a significant relationship between a soil's PWI value and mean annual temperature, allowing for the development of a new temperature proxy. The PWI paleothermometer is effective at reconstructing MAT in Inceptisols, Alfisols, and Ultisols, which correspond to Argissol and Protosol paleosols. By improving upon previous clay-rich paleosol temperature proxies, it further demonstrates the effectiveness of soil-order specific paleosol proxies, and underscores the need for their continued development. The Oregon paleosol PWI record more accurately constrains Cenozoic terrestrial MAT trends, and is in good agreement with the regional paleobotanical record. This revised record allows for more confident comparisons with the deep-marine oxygen isotope record and demonstrates that paleosol climate records are capable of capturing both local and global climate trends.

ACKNOWLEDGMENTS

This manuscript was improved thanks to helpful comments from Steve Driese, two anonymous reviewers, and A.E. William Collins. This work was supported by the National

Science Foundation Graduate Student Research Fellowship under Grant No. DGE 1256260 to TMG, and by National Science Foundation Award No. 1050760 to NDS.

REFERENCES CITED

- Buol, S.W., Southard, R.J., Graham, R.C., and McDaniel, P.A., 2011, Soil genesis and classification: Chichester, West Sussex and Ames, Iowa, Wiley-Blackwell, xvi, 543 p., 12 p. of color plates.
- Chou, L., and Wollast, R., 1984, Study of the weathering of albite at room-temperature and pressure with a fluidized-bed reactor: *Geochimica et Cosmochimica Acta*, v. 48, p. 2205–2217, doi:10.1016/0016-7037(84)90217-5.
- Condie, K.C., 1993, Chemical-composition and evolution of the upper continental-crust—Contrasting results from surface samples and shales: *Chemical Geology*, v. 104, p. 1–37, doi:10.1016/0009-2541(93)90140-E.
- Delgado, A., and Reyes, E., 1996, Oxygen and hydrogen isotope compositions in clay minerals: A potential single-mineral geothermometer: *Geochimica et Cosmochimica Acta*, v. 60, p. 4285–4289, doi:10.1016/S0016-7037(96)00260-8.
- Dworkin, S.I., Nordt, L., and Atchley, S., 2005, Determining terrestrial paleotemperatures using the oxygen isotopic composition of pedogenic carbonate: *Earth and Planetary Science Letters*, v. 237, p. 56–68, doi:10.1016/j.epsl.2005.06.054.
- Gromet, L.P., Dymek, R.F., Haskin, L.A., and Korotev, R.L., 1984, The North-American shale composite—Its compilation, major and trace-element characteristics: *Geochimica et Cosmochimica Acta*, v. 48, p. 2469–2482, doi:10.1016/0016-7037(84)90298-9.
- Jenny, H., 1941, Factors of Soil Formation; A System of Quantitative Pedology: New York and London, McGraw-Hill, xii, 281 p.

- Liu, Z.H., Pagani, M., Zinniker, D., DeConto, R., Huber, M., Brinkhuis, H., Shah, S.R., Leckie, R.M., and Pearson, A., 2009, Global cooling during the Eocene–Oligocene climate transition: *Science*, v. 323, p. 1187–1190, doi:10.1126/science.1166368.
- Mack, G.H., James, W.C., and Monger, H.C., 1993, Classification of paleosols: *Geological Society of America Bulletin*, v. 105, p. 129–136, doi:10.1130/0016-7606(1993)105<0129:COP>2.3.CO;2.
- Marbut, C., 1935, *Atlas of American Agriculture: Part III. Soils of the United States*: Washington, D.C., U.S. Government Printing Office, p. 1–98.
- Meyers, J.A., 2003, Terrestrial Eocene–Oligocene vegetation and climate in the Pacific Northwest, *in* Prothero, D.R., Ivany, L.C., and Nesbitt, E.A., eds., *From Greenhouse to Icehouse: The Marine Eocene-Oligocene Transition*: New York, Columbia University Press, p. 171–185.
- National Climatic Data Center, 2002, *United States Climate Normals, 1971–2000: Climatology of the U.S.*, No. 81.
- Nordt, L.C., and Driese, S.D., 2010a, New weathering index improves paleorainfall estimates from Vertisols: *Geology*, v. 38, p. 407–410, doi:10.1130/G30689.1.
- Nordt, L.C., and Driese, S.G., 2010b, A modern soil characterization approach to reconstructing physical and chemical properties of paleo-vertisols: *American Journal of Science*, v. 310, p. 37–64, doi:10.2475/01.2010.02.
- Óskarsson, B.V., Riishuis, M.S., and Arnalds, O., 2012, Climate-dependent chemical weathering of volcanic soils in Iceland: *Geoderma*, v. 189–190, p. 635–651, doi:10.1016/j.geoderma.2012.05.030.

Parker, A., 1970, Index of weathering for silicate rocks: Geological Magazine, v. 107, p. 501–504, doi:10.1017/S0016756800058581.

Peppe, D.J., and 25 others, 2011, Sensitivity of leaf size and shape to climate: Global patterns and paleoclimatic applications: *The New Phytologist*, v. 190, p. 724–739, doi:10.1111/j.1469-8137.2010.03615.x.

Rasmussen, C., and Tabor, N.J., 2007, Applying a quantitative pedogenic energy model across a range of environmental gradients: *Soil Science Society of America Journal*, v. 71, p. 1719–1729, doi:10.2136/sssaj2007.0051.

Retallack, G.J., 2001, Soils of the Past: An Introduction to Paleopedology: Oxford, Malden, Massachusetts, Blackwell Science, xi, 404 p.

Retallack, G.J., 2005, Pedogenic carbonate proxies for amount and seasonality of precipitation in paleosols: *Geology*, v. 33, p. 333–336, doi:10.1130/G21263.1.

Retallack, G.J., 2007, Cenozoic paleoclimate on land in North America: *The Journal of Geology*, v. 115, p. 271–294, doi:10.1086/512753.

Sheldon, N.D., 2006, Quaternary glacial-interglacial climate cycles in Hawaii: *The Journal of Geology*, v. 114, p. 367–376, doi:10.1086/500993.

Sheldon, N.D., and Tabor, N.J., 2009, Quantitative paleoenvironmental and paleoclimatic reconstruction using paleosols: *Earth-Science Reviews*, v. 95, p. 1–52, doi:10.1016/j.earscirev.2009.03.004.

Sheldon, N.D., Retallack, G.J., and Tanaka, S., 2002, Geochemical climofunctions from North American soils and application to paleosols across the Eocene-Oligocene boundary in Oregon: *The Journal of Geology*, v. 110, p. 687–696, doi:10.1086/342865.

Tabor, N.J., 2007, Permo-Pennsylvanian palaeotemperatures from Fe-Oxide and phyllosilicate $\delta^{18}\text{O}$ values: Earth and Planetary Science Letters, v. 253, p. 159–171,
doi:10.1016/j.epsl.2006.10.024.

Takeuchi, A., Larson, P.B., and Suzuki, K., 2007, Influence of paleorelief on the Mid-Miocene climate variation in southeastern Washington, northeastern Oregon, and western Idaho, USA: Palaeogeography, Palaeoclimatology, Palaeoecology, v. 254, p. 462–476,
doi:10.1016/j.palaeo.2007.06.023.

Turk, J.K., Chadwick, O.A., and Graham, R.C., 2012, Pedogenic Processes, in Huang, P.M., Li, Y., and Sumner, M.E., eds., Handbook of Soil Sciences: Properties and Processes: Boca Raton, CRC Press, p. 1–29.

Wolfe, J.A., 1994, Tertiary climatic changes at middle latitudes of western North America: Palaeogeography, Palaeoclimatology, Palaeoecology, v. 108, p. 195–205, doi:10.1016/0031-0182(94)90233-X.

Yapp, C.J., 2000, Climatic implications of surface domains in arrays of δD and $\delta^{18}\text{O}$ from hydroxyl minerals: Goethite as an example: Geochimica et Cosmochimica Acta, v. 64, p. 2009–2025, doi:10.1016/S0016-7037(00)00347-1.

Zachos, J.C., Dickens, G.R., and Zeebe, R.E., 2008, An early Cenozoic perspective on greenhouse warming and carbon-cycle dynamics: Nature, v. 451, p. 279–283, doi:10.1038/nature06588.

Zhou, J., Poulsen, C.J., Rosenbloom, N., Shields, C., and Briegleb, B., 2012, Vegetation-climate interactions in the warm mid-Cretaceous: Climate of the Past, v. 8, p. 565–576, doi:10.5194/cp-8-565-2012.

FIGURE CAPTIONS

Figure 1. Paleosol weathering index (PWI) values for modern forest soils (circles) compared with the average composition of various parent material rock types (squares). Soils are distinct from parent material in this index with more developed/weathered soils plotting closer to zero and unweathered rocks plotting at or above 60. Average rock chemical composition is from Condie (1993) and Gromet et al. (1984). UCC—upper continental crust. NA-SC—North American shale composite.

Figure 2. Relationship between mean annual temperature (MAT) and PWI values of modern forest soils. The equation of the logarithmic fit is the calibrated paleothermometer. Soils plotted as triangles were excluded from the regression because their MAT fell below 6 °C. S.E.—standard error.

Figure 3. Eastern Oregon paleosol temperature record calculated using the PWI paleothermometer. Temperatures are plotted as a three-point running average, and the dotted lines represent the error window of ± 2.1 °C. The white square is the modern MAT at Helix, OR. Paleosol chemistry data is from Retallack (2007). The deep marine benthic stacked oxygen isotope record provides a record of global climate trends (Zachos et al., 2008). This record is smoothed with a 0.5 Myr running average and a 0.1 Myr step. E-O—Eocene-Oligocene; Q—Quaternary; Po—Pliocene.

¹GSA Data Repository item 2013176, Figures DR1 and DR2 (additional paleosol weathering index [PWI] relationships) and Tables DR1–DR3 (calculation of the PWI coefficient, modern soil data, and paleosol data), is available online at www.geosociety.org/pubs/ft2013.htm, or on request from editing@geosociety.org or Documents Secretary, GSA, P.O. Box 9140, Boulder, CO 80301, USA.

Figure 1.
Gallagher and Sheldon
G34074_Figure1.pdf

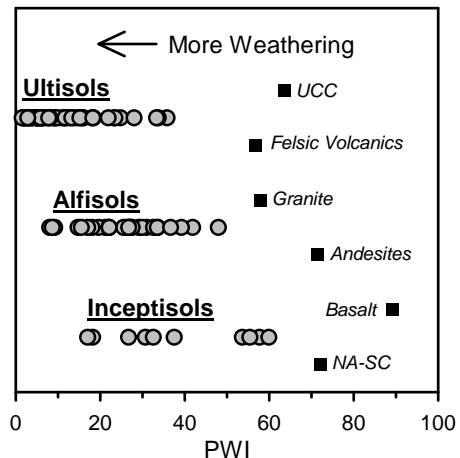


Figure 2.

Gallagher and Sheldon
G34074_Figure2.pdf

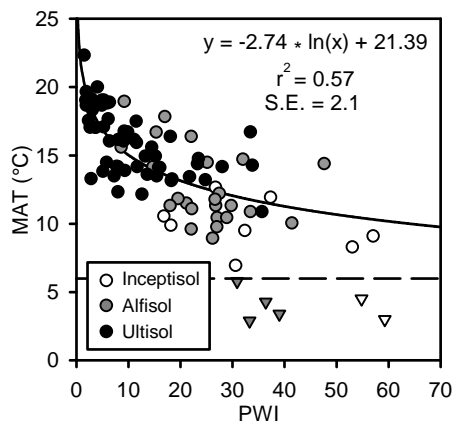
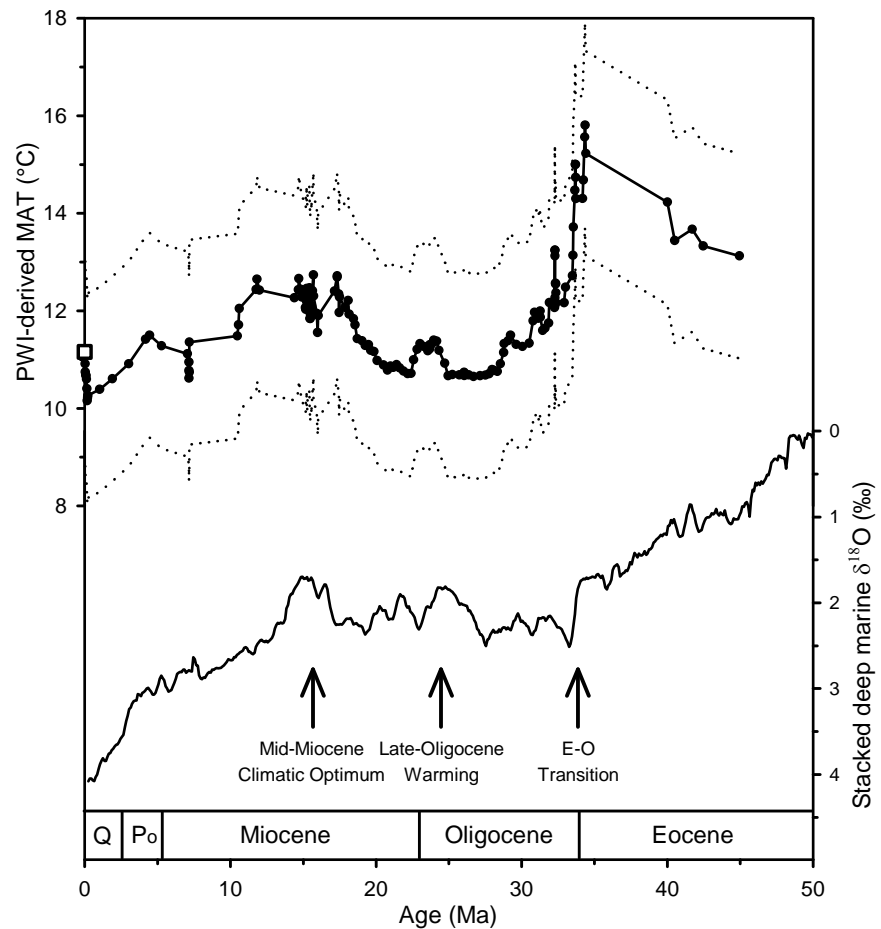


Figure 3.
Gallagher and Sheldon
G34074_Figure3.pdf



Data Repository Item: 2013176

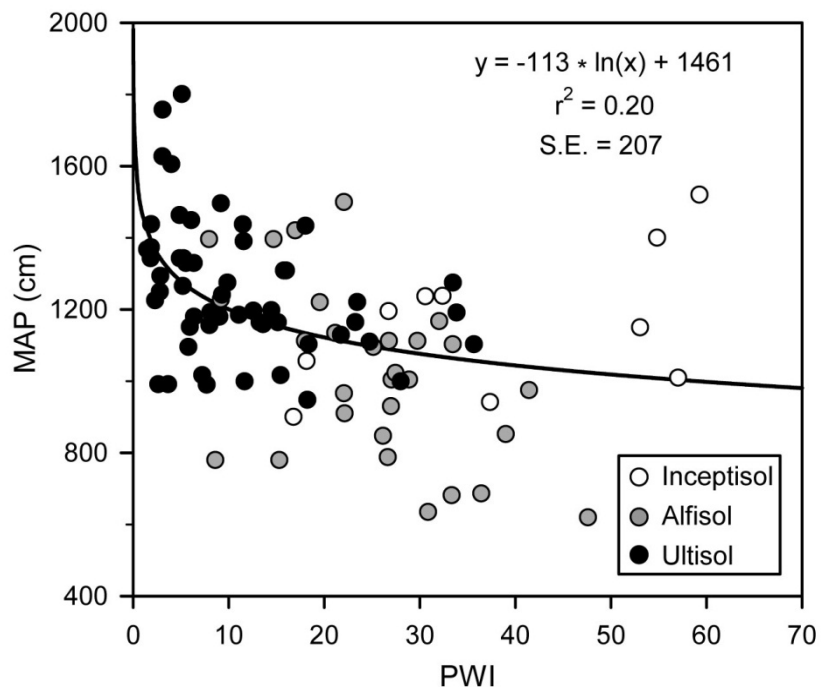


Figure DR1. PWI values for modern soils plotted against mean annual precipitation (MAP).

There is only a weak relationship between the PWI and MAP.

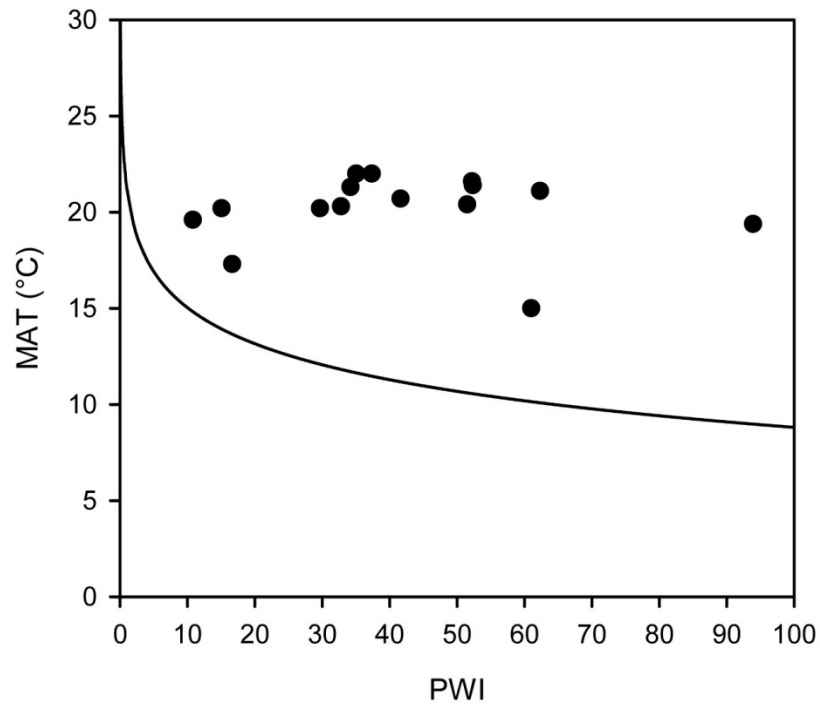


Figure DR2. PWI values for modern Vertisols plotted against MAT. There is no clear relationship between Vertisol PWI values and MAT. The curve shown for comparison is the logarithmic fit of the forest soils against MAT.

TABLE DR1. CALCULATION OF THE PWI COEFFICIENT

Ion	Coordination Number (CN)	Effective Ionic Radius* (r)	Charge (z)	Relative Bond Strength† (RBS)	Electronegativity§ (X)	% Ionic Character# (IC)	PWI Coefficient**
Na ⁺	VIII	1.32	1	0.30	0.93	0.79	4.20
Mg ²⁺	VI	0.86	2	0.89	1.31	0.68	1.66
K ⁺	XII	1.78	1	0.22	0.82	0.82	5.54
Ca ²⁺	VIII	1.26	2	0.63	1.00	0.77	2.05

Note: The cation effective ionic radii were selected according to their most common coordination state. Different coordination states were tested, which had the effect of scaling the coefficients, but not significantly affecting any relationships.

* Shannon (1976).

† $RBS = 2 * z / (r + 1.26)^2$, (Nicholls, 1963).

§ Pauling (1960).

$\%IC = 1 - \exp[-0.25 * (3.44 - X)^2]$, (Pauling, 1960).

** $PWI\ Coeff = 1 / (RBS * IC)$.

TABLE DR2. MODERN SOIL CHEMISTRY DATA

Soil Order	Latitude (°W)	Longitude (°N)	Horizon	CaO	MgO	K ₂ O	Na ₂ O	Reference	PWI	MAT (°C)	MAP (mm)
Inceptisol	77.11	41.27	B	0.36	0.51	1.58	0.80	1	18.13	9.9	1056
Inceptisol	73.13	42.44	B	1.11	0.85	2.60	1.14	1	30.57	6.9	1237
Inceptisol	71.25	42.06	B	1.40	0.77	1.11	2.59	1	32.37	9.5	1238
Inceptisol	82.25	35.44	B	0.24	0.80	3.14	0.60	1	26.70	12.7	1196
Inceptisol	93.62	40.08	B	0.91	1.33	0.78	0.50	1	16.78	10.6	900
Inceptisol	122.59	45.51	B	1.60	1.06	2.17	2.12	1	37.34	11.9	942
Inceptisol	121.62	40.50	B	3.70	3.30	1.30	2.70	3	53.05	8.3	1150
Inceptisol	120.53	38.57	B	5.20	2.70	1.50	3.00	3	59.28	3.0	1520
Inceptisol	120.53	38.57	B	4.70	2.70	1.40	2.70	3	54.83	4.5	1400
Inceptisol	119.32	37.02	B	5.00	3.10	2.00	2.10	3	57.03	9.1	1010
Alfisol	89.61	46.82	B	0.84	0.71	2.20	1.76	1	30.86	5.8	852
Alfisol	92.94	47.43	B	1.87	0.82	1.43	3.01	1	39.02	3.4	682
Alfisol	93.57	47.55	B	1.03	1.66	2.48	1.20	1	33.32	2.9	687
Alfisol	96.53	47.54	B	1.68	1.66	2.51	1.28	1	36.41	4.3	635
Alfisol	86.39	35.84	B	0.18	0.54	0.82	0.04	1	7.92	14.2	1396
Alfisol	87.14	35.58	B	0.48	0.46	1.51	0.32	1	14.70	14.2	1396
Alfisol	77.29	42.85	B	0.59	0.93	2.25	1.02	1	26.13	8.9	848
Alfisol	85.77	39.79	B	1.14	1.59	2.51	1.18	1	33.43	10.9	1103
Alfisol	84.98	39.83	B	0.62	0.92	2.35	1.07	1	27.02	10.4	1005
Alfisol	83.41	39.94	B	2.92	2.56	2.48	0.83	1	41.42	10.1	975
Alfisol	85.57	39.18	B	1.11	1.03	2.03	0.96	1	26.74	11.3	1112
Alfisol	84.98	39.83	B	1.38	1.35	1.92	1.04	1	28.87	10.4	1005
Alfisol	91.17	42.12	B	0.67	1.03	2.03	1.23	1	26.96	9.8	930
Alfisol	84.14	39.12	B	0.43	0.73	1.58	1.07	1	21.12	11.5	1135
Alfisol	85.22	38.21	B	0.71	0.76	1.73	0.54	1	19.50	11.8	1221
Alfisol	85.48	39.34	B	1.32	1.01	2.25	1.11	1	29.74	11.3	1112
Alfisol	85.43	39.21	B	0.44	0.80	1.16	0.93	1	17.97	11.3	1112
Alfisol	81.94	40.81	B	0.33	0.79	2.04	0.83	1	22.05	9.6	966
Alfisol	89.93	32.27	B	0.22	0.51	1.40	0.86	1	16.95	17.8	1421
Alfisol	89.81	33.77	B	0.55	0.02	2.12	1.11	1	22.05	16.4	1500
Alfisol	94.66	31.60	B	0.02	0.80	0.64	0.30	1	9.17	18.9	1228
Alfisol	80.90	35.83	B	1.97	3.96	0.11	1.16	1	32.01	14.7	1168
Alfisol	79.79	36.07	B	2.92	1.25	0.21	1.19	1	25.12	14.5	1096
Alfisol	92.33	38.95	B	0.85	1.23	1.96	1.14	1	27.42	12.2	1023
Alfisol	123.46	42.34	B	1.19	0.57	1.83	1.36	1	26.63	11.8	788
Alfisol	121.62	40.50	B	0.80	1.30	0.50	0.60	3	15.28	16.7	780
Alfisol	120.53	38.57	B	0.40	0.40	0.70	0.20	3	8.58	15.6	780
Alfisol	119.32	37.02	B	0.20	0.70	2.80	0.30	3	22.11	11.1	910
Alfisol	119.32	37.02	B	3.20	1.30	2.20	2.60	3	47.61	14.4	620
Ultisol	76.18	38.41	B	0.74	0.26	1.97	0.44	1	18.34	13.3	1103
Ultisol	75.51	37.90	B	0.20	0.40	1.65	0.49	1	15.40	13.5	1017
Ultisol	76.08	38.77	B	0.40	0.55	2.06	1.09	1	23.23	14.4	1165
Ultisol	75.55	37.89	B	0.22	0.42	0.61	0.16	1	7.21	13.5	1017
Ultisol	76.87	38.78	B	0.30	1.09	2.91	0.30	1	24.73	13.2	1110
Ultisol	75.37	39.71	B	0.19	0.33	0.36	0.56	1	7.97	12.3	1157
Ultisol	74.47	40.16	B	0.46	0.40	1.14	0.38	1	12.56	12.2	1197
Ultisol	77.12	38.90	B	0.22	0.99	2.77	1.01	1	27.99	14.2	999
Ultisol	78.30	38.26	B	0.16	0.37	1.13	0.08	1	9.30	13.9	1241
Ultisol	77.04	38.90	B	0.38	0.53	0.84	0.47	1	11.64	14.2	999
Ultisol	85.69	39.75	B	1.09	1.68	2.70	1.31	1	35.66	10.9	1103
Ultisol	87.14	37.34	B	0.57	0.68	2.09	0.93	1	23.42	14.8	1221
Ultisol	77.97	35.36	B	0.31	0.07	0.40	0.21	1	5.20	13.8	1266
Ultisol	79.68	34.62	B	0.17	0.18	0.16	0.20	1	3.66	17.1	992
Ultisol	81.10	33.82	B	0.10	0.11	0.25	0.00	1	2.30	17.6	1226
Ultisol	77.92	33.72	B	0.00	0.26	0.35	1.67	1	14.45	15.6	1198
Ultisol	79.68	34.62	B	0.27	0.32	0.23	0.00	1	3.65	17.1	992

Ultisol	79.68	34.62	B	0.05	0.04	0.25	0.12	1	2.61	17.1	992
Ultisol	84.19	31.22	B	0.48	0.08	0.18	0.31	1	5.24	19.1	1343
Ultisol	84.19	31.22	B	0.07	0.00	0.17	0.08	1	1.80	19.1	1343
Ultisol	83.98	30.84	B	0.22	0.13	0.04	0.04	1	1.85	19.7	1373
Ultisol	85.39	31.22	B	0.00	0.00	0.11	0.18	1	1.87	18.7	1438
Ultisol	84.78	31.64	B	0.19	0.11	0.43	0.40	1	6.33	18.9	1330
Ultisol	83.25	31.59	B	0.00	0.12	0.55	0.32	1	5.90	18.8	1152
Ultisol	83.59	31.18	B	0.28	0.12	0.04	0.16	1	2.84	19.2	1294
Ultisol	84.09	31.07	B	0.37	0.16	0.18	0.27	1	4.88	19.1	1343
Ultisol	82.20	28.36	B	0.16	0.00	0.12	0.03	1	1.45	22.3	1368
Ultisol	81.25	29.41	B	0.16	0.00	0.17	0.22	1	3.08	18.8	1758
Ultisol	88.71	32.44	B	0.26	0.14	0.37	0.35	1	6.07	17.7	1449
Ultisol	86.96	31.43	B	0.17	0.13	0.32	0.00	1	3.05	18.3	1627
Ultisol	85.11	31.88	B	0.00	0.11	0.22	0.56	1	5.51	18.9	1330
Ultisol	86.62	31.83	B	0.25	0.35	0.30	0.12	1	4.85	18.7	1464
Ultisol	84.28	30.44	B	0.60	0.22	0.15	0.00	1	3.99	20.0	1606
Ultisol	86.35	33.28	B	0.14	0.63	0.81	0.53	1	11.46	17.5	1438
Ultisol	86.86	33.10	B	0.13	0.50	1.06	0.06	1	9.17	16.8	1496
Ultisol	81.96	35.37	B	0.18	0.67	1.40	0.64	1	15.99	14.1	1309
Ultisol	82.04	35.41	B	0.00	0.88	1.66	0.36	1	15.78	14.1	1309
Ultisol	80.77	36.12	B	0.00	0.22	1.07	0.95	1	13.59	13.6	1159
Ultisol	82.65	34.50	B	0.00	0.42	1.10	0.42	1	11.05	16.2	1185
Ultisol	84.20	33.12	B	0.00	0.03	1.28	0.20	1	9.01	16.1	1180
Ultisol	84.30	33.77	B	0.06	0.22	1.16	0.28	1	9.84	16.7	1275
Ultisol	83.67	34.39	B	0.30	0.77	1.11	0.11	1	11.54	15.9	1391
Ultisol	83.50	34.52	B	0.00	0.09	0.80	0.00	1	5.09	13.8	1801
Ultisol	85.19	32.87	B	0.00	1.41	1.69	0.34	1	18.02	16.4	1434
Ultisol	82.74	33.74	B	0.43	0.14	0.73	0.24	1	8.07	16.2	1192
Ultisol	77.83	36.53	B	0.22	0.22	1.65	0.27	1	13.21	14.9	1165
Ultisol	77.79	36.47	B	0.00	0.74	1.71	0.30	1	15.14	14.9	1165
Ultisol	79.66	36.35	B	0.20	0.09	3.99	1.37	1	33.83	14.3	1192
Ultisol	84.17	33.81	B	0.19	0.24	4.94	0.40	1	33.45	16.7	1275
Ultisol	82.81	35.67	B	0.27	0.18	1.25	1.36	1	18.21	13.2	948
Ultisol	84.20	33.12	B	0.09	0.15	0.70	0.20	1	6.35	16.1	1180
Ultisol	79.79	36.07	B	0.39	0.49	0.40	0.00	1	5.77	14.5	1096
Ultisol	94.81	37.11	B	0.77	1.07	1.20	1.10	1	21.73	13.4	1130
Ultisol	121.62	40.50	B	0.30	0.70	0.40	0.20	3	7.69	14.2	990
Ultisol	120.53	38.57	B	0.10	0.30	0.20	0.00	3	2.78	13.3	1250
Mollisol	85.19	40.78	B	1.59	1.53	2.68	0.71	1	32.68	9.9	928
Mollisol	97.18	41.14	B	0.95	0.89	1.90	1.12	1	25.90	10.4	764
Mollisol	92.38	42.45	B	0.80	0.55	1.51	1.25	1	22.54	8.4	842
Mollisol	95.65	40.74	B	1.02	0.69	1.73	1.99	1	30.23	10.5	880
Mollisol	95.65	40.74	B	0.70	1.04	2.08	1.32	1	28.02	10.5	880
Mollisol	95.92	40.97	B	1.03	1.12	2.29	1.14	1	29.57	10.2	855
Mollisol	93.06	41.70	B	0.86	1.33	2.01	0.91	1	26.61	9.6	874
Mollisol	97.37	37.27	B	0.85	0.97	2.32	0.92	1	26.98	13.9	827
Mollisol	97.63	39.82	B	1.18	1.36	2.91	1.14	1	34.75	11.6	785
Mollisol	107.07	52.79	B	8.40	3.13	1.85	1.34	1	63.55	1.6	353
Mollisol	103.67	50.53	B	6.80	2.73	1.77	0.89	1	52.54	2.1	398
Mollisol	96.66	43.98	B	9.61	2.52	1.51	0.96	1	60.89	6.4	602
Mollisol	96.66	43.98	B	9.60	2.90	1.67	0.94	1	63.22	6.4	602
Mollisol	99.38	40.44	B	3.41	1.60	2.81	0.98	1	42.22	9.8	661
Mollisol	98.94	38.52	B	2.15	1.59	2.53	1.40	1	38.72	13.4	672
Mollisol	99.89	38.08	B	2.31	1.52	2.76	1.20	1	38.98	11.6	555
Mollisol	101.83	35.22	B	2.64	1.37	2.48	1.03	1	36.86	13.9	501
Mollisol	100.30	34.01	B	5.07	1.43	2.45	1.02	1	45.74	16.5	612
Mollisol	101.80	33.68	B	14.09	1.67	1.34	0.30	1	68.29	15.4	475
Mollisol	97.59	40.64	B	1.94	1.63	2.52	1.41	1	38.12	10.2	731
Mollisol	96.68	40.81	B	0.96	0.71	1.74	0.88	1	22.63	10.7	755

Mollisol	117.37	47.28	B	1.54	0.99	2.14	1.62	1	33.27	8.3	195
Mollisol	100.89	46.83	B	6.69	2.69	2.28	0.91	1	55.11	5.5	433
Mollisol	103.62	48.15	B	5.79	2.00	2.33	0.91	1	49.27	4.9	360
Mollisol	102.97	41.41	B	4.42	1.60	3.07	1.55	1	51.30	9.1	486
Mollisol	103.66	43.02	B	7.65	1.58	2.17	1.07	1	54.48	8.1	437
Mollisol	104.38	42.03	B	7.44	1.90	2.40	1.06	1	56.32	8.7	352
Mollisol	102.79	46.88	B	3.49	2.24	2.24	1.32	1	44.10	6.1	415
Mollisol	101.05	39.40	B	8.16	1.84	2.55	1.46	1	62.24	10.1	528
Mollisol	102.35	38.82	B	7.78	1.66	1.94	2.46	1	63.35	11.3	406
Mollisol	112.58	39.35	B	14.55	4.34	2.09	1.16	1	91.21	10.1	214
Mollisol	120.53	38.57	B	2.60	1.80	1.00	1.60	3	33.64	17.0	460
Entisol	81.79	26.14	B	1.94	0.03	0.11	0.03	1	8.07	23.4	1318
Entisol	121.62	40.50	B	4.50	6.00	0.90	2.30	3	62.03	6.5	1340
Entisol	119.32	37.02	B	1.30	0.40	4.30	2.80	3	50.66	7.2	1080
Entisol	115.60	30.97	B	4.50	1.70	1.40	4.10	3	59.47	7.4	626
Entisol	115.60	30.97	B	4.20	2.40	2.00	3.00	3	57.33	12.2	454
Entisol	115.60	30.97	B	5.10	2.60	0.70	3.50	3	57.18	17.1	275
Aridisol	105.50	44.29	B	4.37	1.26	2.18	1.54	1	44.42	6.7	435
Aridisol	114.46	42.56	B	10.80	3.41	1.98	1.80	1	77.36	8.6	279
Aridisol	112.58	33.37	B	16.07	1.60	1.80	0.90	1	82.02	21.6	201
Aridisol	114.89	39.25	B	8.61	2.50	2.61	1.26	1	65.65	7.1	253
Aridisol	119.01	43.14	B	9.74	3.30	1.63	2.36	1	74.77	6.8	268
Aridisol	118.58	43.42	B	5.67	2.72	2.54	2.88	1	66.38	6.8	268
Vertisol	96.69	32.83	B	21.98	1.35	1.16	0.18	1	93.89	19.4	941
Vertisol	106.73	32.61	B	9.35	1.63	2.37	0.90	2	60.96	15.0	267
Vertisol	99.50	27.56	B	7.16	1.37	1.46	1.75	2	52.30	21.4	544
Vertisol	97.55	27.56	B	5.09	1.42	1.36	0.72	2	37.32	22.0	755
Vertisol	97.35	28.11	B	3.99	1.41	1.47	0.88	2	35.00	22.0	894
Vertisol	97.12	28.47	B	7.27	2.17	1.72	0.97	2	52.19	21.6	924
Vertisol	97.76	28.72	B	4.84	1.48	0.91	0.74	2	34.16	21.3	1000
Vertisol	96.40	28.88	B	11.08	2.10	1.24	0.86	2	62.26	21.1	1066
Vertisol	96.08	29.43	B	2.95	1.95	1.63	0.65	2	32.77	20.3	1124
Vertisol	95.88	29.60	B	7.42	2.26	1.66	0.78	2	51.46	20.4	1170
Vertisol	95.76	30.51	B	0.51	0.81	0.77	0.16	2	10.79	19.6	1202
Vertisol	95.07	29.59	B	4.30	2.27	1.69	0.98	2	41.59	20.7	1321
Vertisol	94.32	29.87	B	1.37	0.86	0.77	0.29	2	15.04	20.2	1411
Vertisol	94.19	30.04	B	4.07	1.10	0.88	0.75	2	29.66	20.2	1437
Vertisol	88.11	32.40	B	0.13	1.38	1.53	0.22	2	16.62	17.3	1450
Spodosol	73.12	42.36	B	0.64	0.37	3.43	0.57	1	27.85	8.2	1184
Spodosol	67.83	46.13	B	0.19	1.06	1.37	1.32	1	22.06	4.9	1050
Andisol	116.92	47.40	B	1.70	1.31	2.08	1.89	1	36.55	9.0	662
Andisol	120.53	38.57	B	2.90	3.70	0.70	1.40	3	39.44	7.6	1350
Andisol	120.53	38.57	B	3.10	3.80	0.80	1.10	3	39.14	11.3	1300

Note: Reference 1-major element data from Marbut (1935), climatic data from National Climatic Data Center (2002). Reference 2-major element and climatic data from Nordt and Driese (2010). Reference 3-major element and climatic data from Rasmussen and Tabor (2007). Major element data from Reference 1 were measured using wet chemistry techniques, while References 2 and 3 used x-ray fluorescence techniques with comparable error.

TABLE DR3. OREGON PALEOSOL DATA

Locality	Specimen	Age (Ma)	CaO	MgO	K ₂ O	Na ₂ O	PWI	MAT (°C)	MAT 3pt. Avg. (°C)
Helix, OR	JODA9338	0.00	2.61	1.49	2.04	2.11	41.97	11.2	-
Helix, OR	JODA9339	0.02	2.61	1.74	2.09	2.20	43.90	11.0	10.9
Helix, OR	JODA9340	0.04	4.63	1.92	1.87	2.36	51.82	10.6	10.8
Helix, OR	JODA9341	0.06	4.26	2.09	1.80	2.35	50.69	10.7	10.7
Helix, OR	JODA9342	0.09	3.05	2.07	1.91	2.33	46.69	10.9	10.7
Helix, OR	JODA9343	0.12	4.55	2.47	1.82	2.27	52.89	10.5	10.6
Helix, OR	JODA9344	0.13	5.07	2.78	1.66	2.19	54.58	10.5	10.4
Helix, OR	JODA9345	0.16	6.15	2.58	1.85	2.05	57.87	10.3	10.2
Helix, OR	JODA9346	0.18	10.07	2.13	1.61	2.12	69.41	9.8	10.2
Helix, OR	JODA9347	0.21	3.94	2.04	1.83	2.54	50.78	10.6	10.3
Washtucna, WA	JODA9337	1.02	5.47	2.48	2.03	1.94	55.29	10.4	10.4
Washtucna, WA	JODA9336	1.90	6.42	2.32	2.18	2.17	60.55	10.2	10.6
Taunton, WA	JODA9335	3.01	1.76	2.09	2.41	1.59	39.99	11.3	10.9
Richland, WA	JODA9334	4.17	1.42	1.59	2.54	1.90	39.55	11.3	11.4
Richland, WA	JODA9325	4.45	1.39	1.85	2.62	0.99	34.81	11.7	11.5
McKay Reservoir, OR	JODA9320	5.27	3.35	1.80	1.13	1.51	36.53	11.5	11.3
Rattlesnake Creek, OR	JODA7624	7.04	5.35	2.90	0.88	2.00	50.22	10.7	11.1
Rattlesnake Creek, OR	JODA7608	7.15	4.04	1.80	0.82	2.17	41.71	11.2	11.0
Rattlesnake Creek, OR	JODA7634	7.15	3.30	1.69	1.78	2.13	43.92	11.0	10.6
Rattlesnake Creek, OR	JODA7618	7.15	8.97	4.46	0.50	2.65	72.05	9.7	10.8
Rattlesnake Creek, OR	JODA7597	7.17	2.72	2.82	1.38	0.82	35.23	11.6	10.8
Rattlesnake Creek, OR	JODA7603	7.17	1.50	2.90	1.45	2.90	45.60	10.9	11.4
Juntura, OR	JODA9317	10.47	0.93	0.62	3.42	1.55	36.57	11.5	11.5
Juntura, OR	JODA9314	10.56	1.66	0.62	1.57	1.90	30.73	12.0	11.7
Juntura, OR	JODA9312	10.60	2.08	0.91	1.45	2.31	35.53	11.6	12.0
Unity, OR	JODA9246	11.76	1.24	0.76	0.97	1.77	25.36	12.5	12.4
Unity, OR	JODA9231	11.81	1.07	0.84	1.05	0.95	19.98	13.2	12.6
Unity, OR	JODA9225	11.98	1.59	0.99	1.35	1.53	28.20	12.2	12.4
Mascall Ranch, OR	M-02-3d4	14.38	2.91	1.14	0.78	1.85	32.45	11.9	12.3
Mascall Ranch, OR	M-02-1d5	14.66	1.91	1.55	0.76	0.87	23.73	12.7	12.4
Mascall Ranch, OR	M-02-2d4	14.69	1.95	1.34	0.74	0.96	23.50	12.7	12.7
Mascall Ranch, OR	JODA9322	14.80	1.99	1.14	0.95	1.14	25.28	12.5	12.4
Mascall Ranch, OR	M-02-4d4	14.88	2.71	1.74	1.04	1.02	30.10	12.1	12.3
Mascall Ranch, OR	MA46	15.13	2.51	1.61	0.68	1.21	28.00	12.3	12.1
Mascall Ranch, OR	MA45	15.16	3.14	1.43	0.80	1.51	32.30	11.9	12.0
Mascall Ranch, OR	MA44	15.18	2.65	1.42	0.80	1.60	31.08	12.0	12.2
Mascall Ranch, OR	MA41	15.22	0.72	1.57	0.57	1.47	22.41	12.9	12.3
Mascall Ranch, OR	MA40	15.23	1.31	1.76	0.93	1.67	28.82	12.2	12.4
Mascall Ranch, OR	MA39	15.23	1.64	1.48	0.77	1.58	27.32	12.3	12.3
Mascall Ranch, OR	MA38	15.25	2.00	1.50	1.00	1.10	26.82	12.4	12.0
Mascall Ranch, OR	5d2	15.27	3.10	1.18	1.33	2.05	37.90	11.4	12.2
Mascall Ranch, OR	MA36	15.30	2.15	1.50	1.04	0.30	22.18	12.9	12.3
Mascall Ranch, OR	MA32-3	15.43	2.17	1.71	0.78	0.82	25.12	12.5	12.5
Mascall Ranch, OR	MA31-4	15.43	3.08	1.90	0.89	1.00	31.09	12.0	12.3
Mascall Ranch, OR	MA29-1	15.44	2.17	1.62	0.95	0.99	26.90	12.4	12.1
Mascall Ranch, OR	MA28-5	15.45	2.62	1.66	1.14	1.44	32.87	11.8	12.0
Mascall Ranch, OR	MA28-1	15.45	2.88	1.80	1.18	1.23	33.21	11.8	11.8
Mascall Ranch, OR	MA26-3	15.48	3.00	1.74	1.07	1.07	31.67	11.9	11.8
Mascall Ranch, OR	MA26-1	15.48	3.00	1.60	0.90	1.50	33.01	11.8	11.9
Mascall Ranch, OR	MA20-3	15.55	2.17	1.87	1.11	1.17	30.09	12.1	12.0
Mascall Ranch, OR	MA20-1	15.55	2.07	1.79	1.08	1.12	28.88	12.2	12.1
Mascall Ranch, OR	MA18.5	15.56	2.33	1.87	0.99	1.17	29.97	12.1	12.0
Mascall Ranch, OR	MA18-2	15.56	2.71	1.81	1.13	1.24	32.41	11.9	12.1
Mascall Ranch, OR	MA9A2	15.63	2.22	1.96	1.02	0.79	27.54	12.3	12.4
Mascall Ranch, OR	MA6	15.69	1.80	1.60	0.60	0.60	20.76	13.1	12.7
Mascall Ranch, OR	MA4	15.70	2.01	1.51	0.65	0.79	22.74	12.8	12.3
Picture Gorge, OR	JODA9106	15.92	2.53	4.76	1.01	1.39	44.20	11.0	11.9
Picture Gorge, OR	JODA9119	15.98	2.18	2.56	1.28	0.69	30.71	12.0	11.6
Picture Gorge, OR	JODA9128	16.02	2.76	1.96	1.29	1.34	34.83	11.7	11.9
Bone Creek, OR	JODA8385	17.14	2.29	1.53	1.07	1.38	30.31	12.0	12.4
Bone Creek, OR	JODA8354	17.32	1.38	0.90	0.86	0.57	17.67	13.5	12.7
Bone Creek, OR	JODA8358	17.33	1.74	1.40	1.07	0.94	24.79	12.6	12.7
Bone Creek, OR	JODA8378	17.43	2.26	1.32	1.35	1.43	31.33	12.0	12.3
Bone Creek, OR	JODA8364	17.46	1.64	1.34	1.30	0.96	25.66	12.5	12.0
Bone Creek, OR	JODA8372	17.48	2.62	1.30	1.83	1.77	37.69	11.5	12.3
Kimberly, OR	JODA9074	17.85	1.64	1.39	0.94	0.71	22.06	12.9	12.1

Locality	Specimen	Age (Ma)	CaO	MgO	K ₂ O	Na ₂ O	PWI	MAT (°C)	MAT 3pt. Avg. (°C)
Kimberly, OR	JODA9072	18.07	2.70	1.30	1.45	1.28	32.42	11.9	12.2
Kimberly, OR	JODA9070	18.14	2.56	1.17	1.14	1.68	32.26	11.9	11.9
Kimberly, OR	JODA9069	18.44	2.30	1.52	1.09	1.30	29.89	12.1	11.8
Kimberly, OR	JODA9067	18.55	2.67	1.68	1.16	1.85	36.04	11.6	11.7
Kimberly, OR	JODA9066	18.70	2.56	1.19	1.62	1.95	37.00	11.5	11.4
Kimberly, OR	JODA9065	19.02	3.17	1.11	1.86	2.03	40.85	11.2	11.4
Kimberly, OR	JODA9064	19.25	2.45	1.27	1.75	1.96	37.76	11.4	11.3
Kimberly, OR	JODA9063	19.47	2.56	1.36	1.86	2.25	41.14	11.2	11.3
Kimberly, OR	JODA9088	19.61	2.82	1.31	1.75	2.06	39.95	11.3	11.2
Kimberly, OR	JODA9087	19.84	3.09	1.19	1.99	2.23	43.01	11.1	11.2
Kimberly, OR	JODA9086	20.07	2.88	1.22	1.89	2.29	42.18	11.1	11.0
Spray, OR	JODA9084	20.50	2.42	2.62	1.63	2.92	49.01	10.7	10.9
Spray, OR	JODA9083	20.78	2.51	1.84	1.66	3.11	47.59	10.8	10.8
Spray, OR	JODA9082	20.99	2.99	1.83	1.74	2.75	47.33	10.8	10.9
Spray, OR	JODA9081	21.17	2.07	1.70	1.72	2.97	44.81	11.0	10.9
Spray, OR	JODA9080	21.40	3.13	1.82	1.48	3.15	48.98	10.7	10.9
Spray, OR	JODA9079	21.61	2.32	1.96	1.65	2.68	44.41	11.0	10.8
Spray, OR	JODA9078	21.87	2.67	1.29	1.47	3.59	48.04	10.8	10.8
Spray, OR	JODA9077	22.16	2.17	0.95	2.42	3.95	52.84	10.5	10.7
Spray, OR	JODA9076	22.40	2.16	0.86	2.16	3.38	47.04	10.9	10.7
Spray, OR	JODA9075	22.58	3.15	0.79	1.66	3.43	47.77	10.8	11.0
Kimberly, OR	JODA9192	22.82	2.86	1.33	1.74	1.88	38.90	11.4	11.2
Kimberly, OR	JODA9191	23.02	2.68	1.56	1.61	1.70	37.21	11.5	11.3
Kimberly, OR	JODA9190	23.27	3.05	1.24	1.83	2.21	41.99	11.2	11.3
Kimberly, OR	JODA9189	23.56	3.21	1.59	1.35	2.25	41.47	11.2	11.2
Bone Creek, OR	JODA8398	23.68	3.28	1.71	1.46	1.97	40.97	11.2	11.2
Bone Creek, OR	JODA8402	23.69	3.31	1.65	1.48	1.88	40.34	11.3	11.3
Bone Creek, OR	JODA8394	23.80	3.01	2.23	1.09	1.65	37.78	11.4	11.3
Bone Creek, OR	JODA8393	23.97	3.48	2.12	1.16	1.81	40.54	11.3	11.4
Bone Creek, OR	JODA8392	24.16	2.84	2.11	1.09	1.67	36.80	11.5	11.4
Bone Creek, OR	JODA8391	24.32	3.11	1.92	0.99	1.99	38.58	11.4	11.2
RF, Longview Ranch, OR	JODA8423	24.71	3.17	1.62	2.51	2.47	49.76	10.7	10.9
RF, Longview Ranch, OR	JODA8422	24.96	3.43	1.73	1.81	2.78	49.14	10.7	10.7
RF, Longview Ranch, OR	JODA8421	25.24	3.72	1.88	1.90	2.74	51.08	10.6	10.7
RF, Longview Ranch, OR	JODA8419	25.72	3.05	1.45	1.82	3.05	48.49	10.8	10.7
RF, Longview Ranch, OR	JODA8418	26.05	3.84	1.79	1.52	2.85	49.66	10.7	10.8
RF, Longview Ranch, OR	JODA8417	26.06	3.50	1.61	1.42	2.99	48.04	10.8	10.7
RF, Longview Ranch, OR	JODA8416	26.37	3.67	1.74	1.76	3.12	52.07	10.6	10.7
RF, Longview Ranch, OR	JODA8415	26.69	3.18	1.14	1.87	3.22	49.14	10.7	10.7
RF, Longview Ranch, OR	JODA8409	27.15	3.86	1.83	1.52	2.82	49.69	10.7	10.7
RF, Longview Ranch, OR	JODA8408	27.51	3.54	1.91	2.06	2.69	51.15	10.6	10.7
Longview Ranch airport, OR	JODA8431	27.77	2.91	1.43	2.29	2.75	48.63	10.8	10.7
Longview Ranch airport, OR	JODA8429	27.97	2.83	1.27	1.77	3.26	48.07	10.8	10.8
Longview Ranch airport, OR	JODA8428	28.13	3.41	1.48	1.53	2.82	46.67	10.9	10.8
Longview Ranch airport, OR	JODA8427	28.33	3.15	1.65	2.17	2.72	49.50	10.7	10.8
Longview Ranch airport, OR	JODA8426	28.54	2.98	1.52	2.10	2.91	49.22	10.7	10.9
Painted Hills, OR	JODA5619	28.77	2.92	1.37	2.00	1.66	39.33	11.3	11.2
Painted Hills, OR	JODA5623	28.79	2.89	1.25	2.06	1.56	38.40	11.4	11.3
Painted Hills, OR	JODA5609	29.07	2.85	1.21	2.30	1.68	40.31	11.3	11.4
Painted Hills, OR	JODA5602	29.24	2.75	0.81	1.92	1.80	36.88	11.5	11.5
Painted Hills, OR	JODA5586	29.62	2.25	0.66	2.04	1.61	33.85	11.7	11.3
Painted Hills, OR	JODA5668	30.05	2.74	1.32	2.43	2.92	49.53	10.7	11.3
Painted Hills, OR	JODA5551	30.51	2.55	1.13	2.06	1.87	38.76	11.4	11.3
Painted Hills, OR	JODA5536	30.78	2.97	1.07	0.77	1.71	31.38	11.9	11.8
Painted Hills, OR	JODA5531	30.89	2.54	1.25	0.75	1.64	29.96	12.1	12.0
Painted Hills, OR	JODA5505	31.06	2.68	1.38	0.70	1.84	32.06	11.9	12.0
Painted Hills, OR	JODA5472	31.15	2.64	1.20	0.79	1.84	31.71	11.9	11.8
Painted Hills, OR	JODA5442	31.27	3.65	0.96	0.48	2.04	33.94	11.7	12.0
Painted Hills, OR	JODA5437	31.28	2.32	0.87	0.91	1.44	27.17	12.3	11.9
Painted Hills, OR	JODA5416	31.44	3.67	0.83	0.92	2.10	36.47	11.5	11.6
Painted Hills, OR	JODA5392	31.60	0.95	0.63	6.20	0.45	45.58	10.9	11.6
Clarno, OR	JODA5121	31.85	2.11	0.62	0.92	1.51	25.91	12.5	11.8
Painted Hills, OR	JODA5367	31.90	2.56	0.92	1.33	1.69	32.42	11.9	12.2
Painted Hills, OR	JODA5694	32.25	2.52	0.59	0.71	1.92	28.83	12.2	12.1
Painted Hills, OR	JODA5692	32.26	2.49	0.57	0.83	1.87	29.00	12.2	12.1
Painted Hills, OR	JODA5681	32.26	2.66	0.50	0.86	1.88	29.58	12.1	12.1
Painted Hills, OR	JODA5350	32.28	2.49	0.56	0.85	2.04	30.23	12.0	13.2

Locality	Specimen	Age (Ma)	CaO	MgO	K ₂ O	Na ₂ O	PWI	MAT (°C)	MAT 3pt. Avg. (°C)
Painted Hills, OR	JODA5713	32.28	0.70	0.26	0.26	0.47	8.34	15.5	13.1
Painted Hills, OR	JODA5717	32.28	2.98	0.63	1.40	1.75	33.58	11.8	13.2
Painted Hills, OR	JODA5691	32.28	2.26	0.70	0.69	1.70	26.72	12.4	12.3
Painted Hills, OR	JODA5688	32.32	2.09	0.79	0.71	1.35	24.22	12.6	12.6
Painted Hills, OR	JODA5685	32.33	1.68	1.02	1.33	0.89	24.19	12.6	12.5
Painted Hills, OR	JODA5684	32.34	2.36	0.88	0.62	1.68	27.28	12.3	12.4
Painted Hills, OR	JODA5682	32.36	2.48	0.86	0.84	1.75	29.41	12.1	12.2
Painted Hills, OR	JODA5279	32.92	2.49	0.56	1.15	1.80	30.37	12.0	12.2
Painted Hills, OR	JODA5267	33.01	2.70	0.45	1.06	1.37	27.24	12.3	12.5
Painted Hills, OR	JODA5218	33.48	1.68	0.35	1.15	0.94	20.72	13.1	12.7
Painted Hills, OR	JODA5203	33.52	2.42	0.75	0.83	0.98	23.46	12.7	13.1
Painted Hills, OR	JODA5200	33.55	1.08	0.47	1.14	0.69	17.26	13.6	13.7
Painted Hills, OR	JODA5175	33.65	0.89	0.17	0.31	0.77	10.99	14.8	14.4
Painted Hills, OR	JODA5170	33.68	1.03	0.14	0.61	0.34	10.23	15.0	15.0
Painted Hills, OR	JODA5166	33.69	0.85	0.13	0.60	0.37	9.68	15.1	15.0
Painted Hills, OR	JODA5163	33.71	1.09	0.26	0.62	0.34	11.01	14.8	14.7
Painted Hills, OR	JODA5157	33.72	1.32	0.69	0.36	0.57	13.65	14.2	14.3
Painted Hills, OR	JODA5139	34.18	1.75	1.44	0.10	0.40	15.62	13.8	14.3
Painted Hills, OR	JODA5147	34.23	0.96	0.35	0.17	0.74	10.96	14.8	14.6
Painted Hills, OR	JODA5658	34.32	0.98	0.00	0.29	0.55	9.02	15.3	15.5
Painted Hills, OR	JODA5652	34.35	0.73	0.00	0.20	0.31	5.95	16.4	15.7
Painted Hills, OR	JODA5642	34.40	1.15	0.00	0.27	0.39	8.42	15.5	15.2
Clarno, OR	JODA5048	40.00	1.63	1.12	0.49	0.52	16.98	13.6	14.2
Clarno, OR	JODA5105	40.50	2.13	0.52	0.63	0.61	17.77	13.5	13.4
Clarno, OR	JODA4195	41.71	1.44	0.82	0.98	0.82	19.96	13.2	13.6
Clarno, OR	JODA4161	42.45	1.08	0.02	0.69	0.75	13.17	14.3	13.3
Clarno, OR	JODA5064	44.95	0.90	1.33	0.70	1.90	25.76	12.5	13.1
Clarno, OR	JODA5057	45.00	0.76	1.33	0.63	1.92	24.97	12.6	-

Note: Age and Major Element Data from Retallack (2007)